OPTIMIZATION OF SIMULTANEOUS NON-INTERFERING ROTORCRAFT APPROACH TRAJECTORIES

S. Hartjes, H.G. Visser and M.D. Pavel,
Delft University of Technology, Delft, The Netherlands

Abstract

This study is concerned with the synthesis of rotorcraft-specific Simultaneous Non-Interfering approach trajectories that minimize the noise impact in communities surrounding an airport. Simultaneous Non-Interfering procedures, which are currently being explored in both Europe and the US, allow rotorcraft to fly terminal area trajectories that do not interfere with the fixed-wing IFR traffic flows. For the synthesis of the optimized rotorcraft noise abatement procedures use has been made of an adapted version of NOISHHH, a trajectory optimization toolset that was originally conceived for fixed-wing aircraft applications. The NOISHHH framework combines a noise model, an emissions inventory model, a geographic information system and a dynamic trajectory optimization algorithm to generate routings and flight-paths to minimize noise exposure in residential communities close to the airport. The effectiveness and flexibility of the developed tool is illustrated in numerical examples that demonstrate the optimization of approach trajectories to a helispot located on a major hub airport, for a variety of different environmental criteria.

1. INTRODUCTION

The concept of Simultaneous Non-Interfering (SNI) approaches for rotorcraft is currently being explored in both Europe and the US. The SNI concept was initially developed in the US to enable the integration of both fixed wing and rotorcraft into the terminal airspace system with the aim to reduce delays and increase capacity [1]. It comprises primarily specific IFR departure and approach procedures which enable rotorcraft to operate independently from fixed-wing traffic IFR streams. Due to the much lower approach speeds of helicopters, sequencing helicopter operations into a single IFR approach stream tends to result in congestion and undesirable delays. At present helicopter operators often prefer to operate under VFR to avoid complex IFR procedures, but clearly this does not provide a reliable air transport service in all weather conditions. Also in Europe research pertaining to SNI operations is well underway, notably in the 6th framework project OPTIMAL [2]. The main aim of the OPTIMAL project is to increase airport capacity and efficiency, whilst reducing the noise footprint.

A downside of the SNI concept is that newly developed SNI routes will be located in previously unused airspace, and consequently may overfly noise-sensitive communities that were not affected by air traffic movements before. This, coupled with the fact that helicopter approach operations tend to be relatively noisy, indicates a clear need for optimization of the SNI routes and flight paths such as to reduce the noise impact in the affected residential communities.

Optimization of SNI approaches with respect to community noise impact was first explored by Xue et al. In [3,4], Xue et al present an optimization technique for segmented three-dimensional SNI trajectory design based on an incremental search strategy that combines a *k-ary* tree with Dijkstra's algorithm. The objective function is based on a validated rotorcraft noise model as well as terminal area population density data. Fixed-wing airspace corridors were treated as impenetrable obstacles. In this approach a trajectory is described as a sequence of trimmed flight segments that connect initial approach and landing sites. The number of segments considered in this study remains limited (typically five or less) primarily due to the fact that the computational load increases rapidly with the number of segments. To make the approach numerically tractable a number of simplifying assumptions were introduced. In particular, it was assumed that transitions between trim states do not appreciably affect solution cost.

In [5] a study is presented that deals with generating minimum noise footprints for rotorcraft departure or arrival tracks by wrapping an optimizer around the Rotorcraft noise model RNM, a high-fidelity simulation program that predicts how sound will propagate through the atmosphere and accumulate at observer points located on the ground. In this approach, a trajectory comprises several segments that are parameterized and an optimization algorithm is used to select the parameters such as to minimize the noise footprint.

In comparison to rotorcraft, the optimization of noise abatement procedures for fixed wing aircraft has received considerably more attention. In [6] an optimization approach is presented that, similar to [3,4], relies on segmented routes. The segmented routes, optimized using a genetic algorithm, enable a specification of simple procedures that are amenable to fast on-line computer solutions that can be readily implemented in a guidance system. In [7,8] noise-optimized approach and departure trajectories are computed based on a direct numerical optimization technique that enables to generate (piecewise) continuous optimal trajectories for a point-mass modeled fixed-wing aircraft. The numerical tool that has been used in these particular studies is called NOISHHH. The NOISHHH tool essentially combines a

noise model, a dose-response relationship, an emission inventory model, a geographic information system, and a dynamic trajectory optimization algorithm. NOISHHH generates routings and flight-paths for both arrivals and departures that minimize the environmental impact in the residential communities surrounding the airport, while satisfying all imposed operational and safety constraints.

In [9] an effort is reported that is aimed at extending the NOISHHH tool to permit the computation of noise-optimized SNI trajectories for rotorcraft. This extension does not only concern a modification of the dynamic vehicle model and the operational context, but also entails an adaptation of the implemented noise model, based on the Integrated Nose Model INM 6.2. [10].

The study presented herein builds on [9], introducing a significantly more sophisticated and comprehensive acoustic methodology based on the Integrated Noise Model INM 7.0a [11]. The environmentally optimized SNI trajectories calculated with the rotorcraft version of NOISHHH are illustrated in an example scenario involving a hypothetical SNI instrument approach of a Robinson R22 helicopter [9] to a helispot located on runway 22 of Amsterdam Airport Schiphol (AAS) in the Netherlands.

2. ENVIRONMENTAL OPTIMIZATION

To date a variety of noise abatement procedures has been proposed. Quite often, noise abatement procedures are designed to minimize the area impacted by high-intensity aircraft noise. Although the application of a procedure that is designed in this fashion may indeed result in a reduction in the area impacted by high-intensity noise, it is readily clear that an exposed area criterion can hardly be viewed as a metric for the true noise impact experienced by the residents in the exposed communities surrounding an airport. By basing noise abatement procedure design on environmental criteria that directly reflect the noise impact in the affected communities, it can be much better assured that air traffic is routed over less noise-sensitive areas.

In this study a range of environmental performance criteria has been considered, including both generic criteria and site-specific criteria that depend on the actual population density distribution in the neighborhood of the considered landing site. To demonstrate a trade-off between the various environmental criteria, a composite performance measure is considered that consists of a weighted combination of four relevant indicators:

$$J = Fuel + K_1 \cdot Awak + K_2 \cdot Pop_{65dB} + K_3 \cdot Area_{65dB} , \quad (1)$$

where *Fuel* is the fuel-consumed, *Awak* is the number of people within the exposed community that is expected to awake due to a single event nighttime flyover, Pop_{65dB} is the population living within the 65dB(A) level contour, and $Area_{65dB}$ is the total area enclosed within the 65 dB(A) contour (footprint). The parameters K_i (≥ 0) are the user-selected weighting factors in the composite performance index. If so desired, a reference noise level different from 65 dBA can be selected. It is also possible to extend the performance index (1) to include multiple noise level criteria.

The specification of an awakening-related performance index requires knowledge of the relationship between aircraft noise exposure and sleep disturbance. In NOISHHH the dose-response relationship as proposed by the Federal Interagency Committee on Aviation Noise in 1997 has been implemented [7-9]. The 1997 curve, shown in Fig. 1, can be represented by the following relationship for the percentage of the exposed population expected to be awakened *(%Awakenings*) as a function of the exposure to single event noise levels expressed in terms of sound exposure level:

$$\%Awakenings = .0087 \, (SEL - 30)^{1.79} , \quad (2)$$

where *SEL* is defined as the Sound Exposure Level (dB) that is experienced indoors. The proposed relationship represents a worst-case bound on the number of people likely to awake. It needs to be cautioned that the FICAN relationship has been established using data from field trials in which the population was exposed to flyovers of fixed wing jet aircraft. Evidently, this sleep disturbance relationship does not necessarily have to be representative for helicopter flyovers.

In this study, indoor sound levels at observer locations are obtained by lowering the computed outdoor sound levels at those locations by a representative value for transmission loss for a typical home with the windows closed [7-9]. The methodology for calculating the outdoor noise exposure from each individual aircraft flyover that has been adopted in NOISHHH is based on the well-known Integrated Noise Model INM [10,11]. By combining the *%Awakenings* results with the actual population density distribution in the noise-exposed residential communities, the absolute number of people likely to awake due to a single night-time flyover can be determined [7-9].

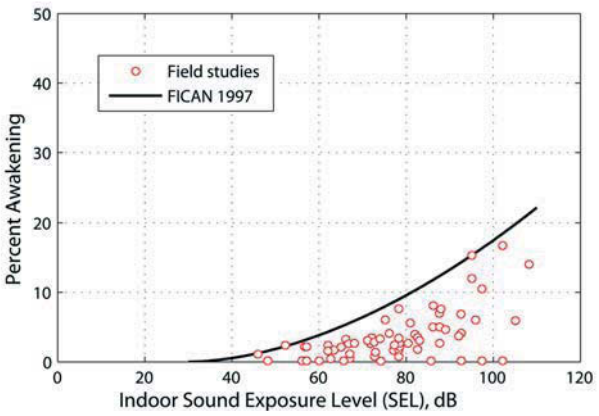

FIGURE 1. FICAN proposed sleep disturbance dose-response relationship [7-9].

The Integrated Noise Model INM has been the Federal Aviation Administration's (FAA) standard methodology for noise assessments since 1979. It has been developed through a succession of versions, currently at version 7.0.

In the U.S.A., INM is typically used for noise compatibility planning and for Environmental assessments and Environmental Impact Statements under FAA order 1050 [12].

Helicopter noise modeling was first introduced in INM version 6.0. The earliest version of INM that was implemented in the NOISHHH tool for rotorcraft procedures design is version 6.2, which in comparison to version 6.0, contains an extensive set of rotorcraft flyover noise curves [10]. In contrast to the most recent INM version (7.0a), which includes detailed modeling of helicopter noise based on the FAA's Heliport Noise Model (HNM Version 2.2) [11], INM version 6.2 only provides partial implementation of HNM helicopters as fixed-wing aircraft. For example, INM 6.2 models a helicopter as an omni-directional point source and, as a consequence, the noise levels on either side of the helicopter track may not be accurately estimated.

Through the integration of HNM, extensive new helicopter noise modeling capabilities and associated adjustments are added to INM 7.0, including helicopter-specific noise-power-distance (NPD) data advancing tip Mach number, lateral directivity, static directivity and static duration adjustments. INM7.0a is the most recent release of INM, primarily aimed at correcting minor software issues encountered in INM7.0.

In the present study, optimal trajectories have been computed using INM 6.2 as well as INM 7.0a. As will be demonstrated, the application of the two different INM noise models leads to significantly different results. A more general, detailed comparison between the two INM versions is presented in [13].

All INM versions use tabulations of Noise-Power-Distance (NPD) relationships for specific reference conditions for each aircraft or rotorcraft type considered. These give, for a specific aircraft speed, A-weighted *SEL* versus slant range from observer to aircraft/rotorcraft as a function of engine thrust settings. In the case of aircraft the thrust settings are related to aircraft engine power states, but for rotorcraft the thrust settings are related to the helicopter flight path angles. There are three helicopter types in INM with expanded NPD data sets. One of the types for which an extended set of NPD curves is available is the Robinson R22. This particular helicopter type has been selected in the present study.

INM 7.0a contains three SEL curves per operational mode for noise exposure to the left, center and right of the flight track. In contrast, INM 6.2 can only model symmetrical noise relative to the flight track, and for this reason the three original HNM curves were energy-averaged to obtain a single NPD curve per flight mode.

From the set of NPD curves available for the Robinson R22 helicopter, noise curves are extracted for four different operational modes. Three (sets of) curves represent approach (APP) mode and one (set) represents level flyover (LFO). The SEL noise curves for the Robinson R22 helicopter are shown in Figure 2 for descent angles of 3°, 6°, 9°, and LFO of 0°. Further details can be found in [9]. The NPD data are used to either interpolate or extrapolate an associated noise-level value. The interpolation/extrapolation is a piecewise linear process between the flight path angle and the base-10 logarithm of the distance. However, interpolation and extrapolation between the left, center and right NPD curves are handled using the lateral directivity adjustment in INM 7.0a [11]

In NOISHHH sound exposure levels are computed on observer locations that are arranged in the form of a rectangular grid of points surrounding the residential areas in the vicinity of the approach path. The size and mesh of the grid have a significant impact on the computational burden of the iterative optimization process and must therefore be judiciously chosen for each specific case. The numerical example presented in this paper is based on an SNI approach to runway 22 of AAS. Figure 3 illustrates a typical example of such a SNI approach within the Schiphol control region (CTR), a zone operated by tower control. To be able to capture the noise impact for this particular approach a rectangular grid of relatively large size (25×20 km^2) was adopted. To mitigate the computational burden, a relatively large cell size (1×1 km^2) was employed. Note that the observer (noise calculation) points are located at the centers of the grid cells. The grid adopted for the noise calculations is also used to define the population distribution (see Figure 3).

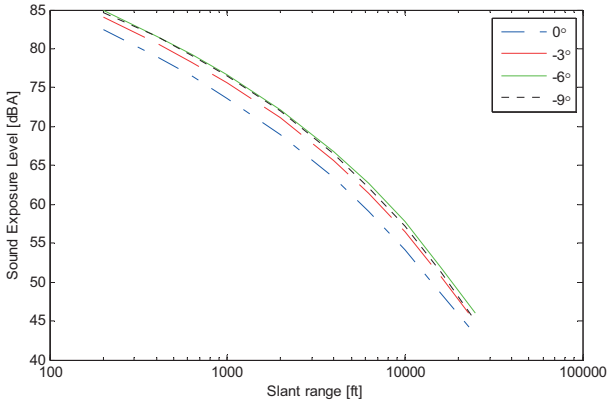

FIGURE 2. INM 6.2 NPD curves for various values of flight path angle (Robinson R22).

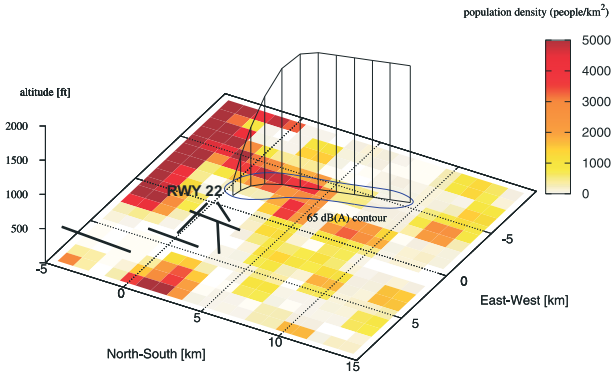

FIGURE 3. SNI trajectory within the Schiphol CTR with underlying noise/population grid area.

To assess the difference in the noise impact of the two considered INM versions, some study runs were conducted prior to the noise optimization trials. In the study runs, the same fuel-optimized trajectory was considered to evaluate the SEL metrics in both versions 6.2 and 7.0. The results from these studies are plotted as contours and compared In Figure 4.

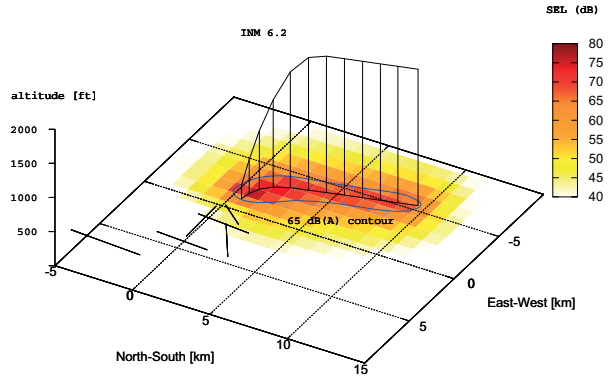

a) INM 6.2 footprint

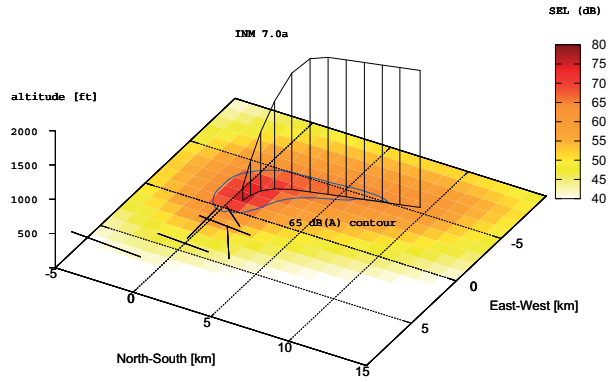

b) INM 7.0a footprint

FIGURE 4. Comparison of INM 6.2 and 7.0a footprints for a representative SNI approach trajectory.

The SNI approach trajectory considered in Figure 4 is identical to the trajectory shown in Figure 3. A comparison between the two 65dB(A) contours in Figure 4 reveals some significant differences. In addition to the clearly visible effects of reduced lateral attenuation and asymmetrical directivity associated with INM 7.0, it can also be observed that the exposed area close to the terminal point of the trajectory is significantly increased, whilst the exposed area near the initial point is reduced in the INM 7.0a footprint. The overall increase in the 65 dB(A) footprint area size is some 27% and the increase in the population enclosed within the 65 dB(A) contour is close to 9%.

3. HELICOPTER PERFORMANCE MODELING

The NOISHHH tool does not rely on the flight-path computation methodology implemented in the INM package, but rather makes use of a simplified point-mass helicopter model in three-dimensions [14,15]. The calculations are performed in standard atmospheric conditions, and it is assumed that no wind is present in this study. A local horizontal (NED) reference frame has been used to formulate the three-dimensional point-mass equations of motion:

$$
\begin{aligned}
\dot{u} &= (C_x \rho(\Omega R)^2 \pi R^2 - f_e \frac{1}{2} \rho u V)/m \\
\dot{v} &= (C_y \rho(\Omega R)^2 \pi R^2 - f_e \frac{1}{2} \rho v V)/m \\
\dot{w} &= (C_z \rho(\Omega R)^2 \pi R^2 - f_e \frac{1}{2} \rho w V - mg)/m \\
\dot{x} &= u \\
\dot{y} &= v \\
\dot{h} &= w
\end{aligned}
\qquad (3)
$$

where:

$$V = \sqrt{u^2 + v^2 + w^2} \quad , \qquad (4)$$

is the magnitude of the velocity vector (airspeed) of the helicopter. Also note that in Eqs. (3), f_e represents the equivalent flat plate area, Ω is the rotor angular speed, and R is the rotor radius. It is assumed that the helicopter mass m remains constant throughout the flight. The thrust coefficients C_x, C_y, C_z can be readily related to thrust T and thrust inclination angles β_{long}, β_{lat} (see Figure 5) through:

$$
\begin{aligned}
C_x &= C_T \sin(\beta_{long}) \cos(\beta_{lat}) \\
C_y &= C_T \sin(\beta_{long}) \sin(\beta_{lat}) \\
C_z &= C_T \cos(\beta_{long})
\end{aligned}
\qquad (5)
$$

where:

$$C_T = T / \rho(\Omega R)^2 \pi R^2 \qquad (6)$$

is the thrust coefficient. The controls in the point-mass helicopter model are C_x, C_y, C_z. The required power coefficient C_P is obtained from the following relation [14,15]:

$$C_P = C_T \sqrt{\frac{1}{2} C_W} (K_{ind} \bar{v}_i + \bar{U}_c) + \frac{1}{8} \sigma c_d (1 + 4.65 \mu^2) \quad , \qquad (7)$$

where:

$$C_W = W / \rho(\Omega R)^2 \pi R^2 \qquad (8)$$

is the thrust coefficient in hover, K_{ind} is the induced-power factor, $\bar{v}_i$ is the normalized induced velocity, $\bar{U}_C$ is the

normalized velocity component perpendicular to the tip path plane of the rotor, σ is the solidity of the rotor, c_d is the mean profile drag coefficient of the rotor-blades, and μ is the rotor advance ratio.

Note that the main rotor power required is taken as the sum of induced power, climb power and profile power. Although engine power should include tail rotor power and installation losses, these are secondary effects and have not been considered in NOISHHH. The power required P_{req} by the helicopter should not exceed the available power P_{avail}:

$$P_{req} = C_P \rho (\Omega R)^3 \pi R^2 \leq P_{avail} \quad (9)$$

The fuel flow is defined as the product of the Specific fuel-consumption *SFC* and the required power [16]:

$$\dot{m}_{fuel} = SFC \cdot P_{req} \quad (10)$$

The R22 features an *SFC* value of 0.44 lb/hp/hr or $7.43449062 \cdot 10^{-8}$ kg/W/s [17].

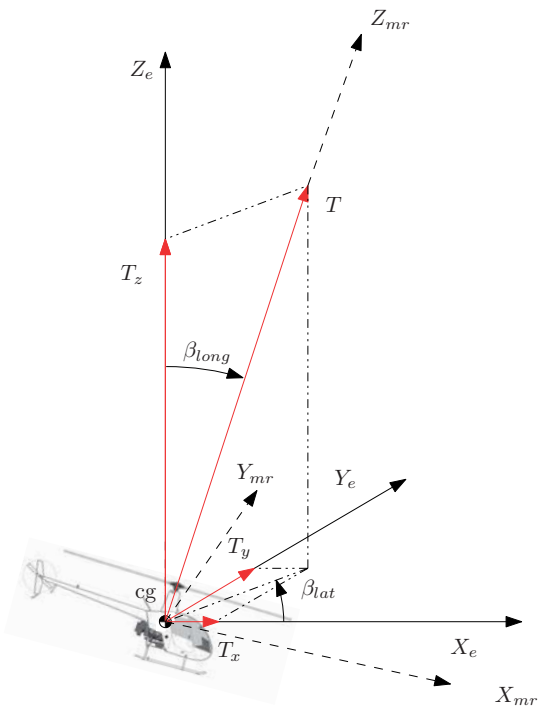

FIGURE 5. Thrust vector decomposed along the axes of the NED reference frame ($-\pi \leq \beta_{lat} \leq \pi$; $0 \leq \beta_{long} \leq \beta_{max}$)

In addition to the above power limit, a variety of performance constraints, passenger comfort and other operational constraints has been included in the SNI approach problem formulation. These constraints have been summarized in Table 1. Note that the permissible range for the flight path angle has been set at [-9°, 0°] in order to remain within the value range of the INM noise database. The constraint set also includes constraints on the range of permissible accelerations/decelerations. In this numerical example fairly tight limits on the lateral, longitudinal and vertical acceleration have been assumed. In particular, the imposed constraint on lateral acceleration limits the bank angle of the helicopter to just a few degrees.

In this study, a model of the Robinson R22 helicopter has been utilized. Details regarding the numerical values of the model parameters and constraint limits in Table 1 can be found in [9].

TAB 1. Overview of trajectory and control constraints for SNI approach.

constraints	Inequality
Never exceed speed	$\sqrt{u^2+v^2+w^2} \leq V_{n.e.}$
Maximum level speed	$\sqrt{u^2+v^2} \leq V_{xy,\max}$
Maximum rate of descent	$-800\,fpm \leq w \leq 0$
Max/min flight path angle	$\sin(\gamma_{\min}) \leq \frac{w}{\sqrt{u^2+v^2+w^2}} \leq 0; \gamma_{\min} = -9^\circ$
Max acceleration/deceleration	$\sqrt{(\dot{u})^2+(\dot{v})^2+(\dot{w})^2} \leq 0.05 g_0$
Maximum thrust coefficient	$\sqrt{C_x^2+C_y^2+C_z^2} \leq C_{T,\max}\frac{\rho_{msl}}{\rho}$
Rotor upward thrust	$C_z \geq 0$
Performance constraint	$P_{available} \geq P_{req}$

4. NUMERICAL METHOD

The numerical trajectory optimization method implemented in NOISHHH is the direct optimization technique of collocation with nonlinear programming (NLP). The collocation method essentially transforms an optimal control problem into a NLP formulation by discretizing the trajectory dynamics [7-9]. To this end, the time interval of an optimal trajectory solution is divided into a number of subintervals. The individual time points delimiting the subintervals are called nodes. The values of the states and the controls at the nodes are then treated as a set of NLP variables. The system differential equations are discretized and transformed into algebraic equations (implicit integration). The path and control constraints imposed in the original optimal control problem are treated as algebraic inequalities in the NLP formulation. To solve the described optimal control problem, a software package called EZopt has been used [7-9]. The collocation approach adopted in EZopt results in piecewise constant control histories and piecewise linear state histories. This

renders EZopt fully compatible with the discretization (segmentation) approach taken in the INM.

Generally, the accuracy of the numerical solution of the problem improves with an increasing number of subintervals, or equivalently, the number of nodes. On the other hand, increasing the number of nodes requires a larger computational effort, hence forcing a compromise between desired accuracy and computational burden. In the NOISHHH context, the adopted flight path segmentation is primarily based on the requirements associated with the computational methodology employed in the INM model. In the present study, the overall time interval is nominally divided into 20 non-equidistant subintervals, yielding an NLP problem of 262 NLP variables and 418 non-linear constraints.

5. EXAMPLE SCENARIO AND SNI PROCEDURE DESIGN

In the example scenario a hypothetical SNI instrument approach from the South to the helispot located on runway 22 of AAS has been selected. The instrument approach procedures presently in use at AAS are optimized for fixed-wing aircraft. The geometry and speed profile of the instrument procedures introduced here are adapted to rotorcraft capabilities and are designed to avoid existing fixed-wing traffic corridors. The resulting approach procedures are suitable for rotorcraft only. At present no regulations for specific SNI rotorcraft approach procedures are in place. The procedure design conducted in this study therefore merely provides examples of possible rotorcraft procedures. The NOISHHH tool has been set up in a generic way, allowing to specify approach procedures in terms of initial and final conditions, number and type of approach procedure segments (not to be confused with INM segments!), navigation system requirements, fixed-wing traffic corridor constraints, and operational limitations (e.g., the items listed in Table 1). To implement the various procedure segments, a so-called multi-phase optimization procedure is employed in NOISHHH [7-9]. A multi-phase formulation allows the implementation of different sets of constraints for different flight phases.

Figures 3 and 4 show a typical example of a fuel-optimized approach trajectory generated with the newly developed rotorcraft-specific NOISHHH version. The trajectory comprises two segments only. The initial approach segment starts at a given altitude of 2,000 ft, at the boundary of the control zone. However, the initial heading and speed are not specified, but have been determined in the optimization process, governed by various operational constraints. The final approach segment starts at a specified altitude of 500 ft and ends at the decision height of 200 ft. The final approach segment is assumed to be flown in a fixed direction along the localizer (heading 280°) and glide slope. The value of the glide slope angle is not specified but also determined in the optimization process. The final speed is again not specified, but selected through optimization within the operational constraints (which includes a minimum speed of 30 kts). A maximum descent rate limit of 800 fpm is imposed throughout the approach. However, at the terminal point (decision altitude), the descent rate limit is reduced to 500 fpm.

6. NUMERICAL RESULTS

To investigate the characteristics of optimal SNI approach trajectories, a parametric investigation involving the weighting parameters in the composite noise performance index given by Eq.(1) is conducted. All presented approach trajectories feature two segments and are initiated at an altitude of 2,000 ft. The final approach phase is commenced at an altitude of 500 ft, resulting in a fairly short localizer/glide slope phase. The major results obtained using INM 6.2 for four selected cases are summarized in Table 2. Each of the four selected cases is represented by a different set of weighting factors K_i (i=1,2,3) in Eq.(1). The minimum-fuel formulation, with all weighting factors set to zero, is selected as a reference case (case 1). In the cases 2 through 4, only to one of the three weighting factors a positive value is assigned. In each of these three cases the positive weighting factor is given a fairly large value, in order to ensure that the optimal solution is not dominated by fuel considerations.

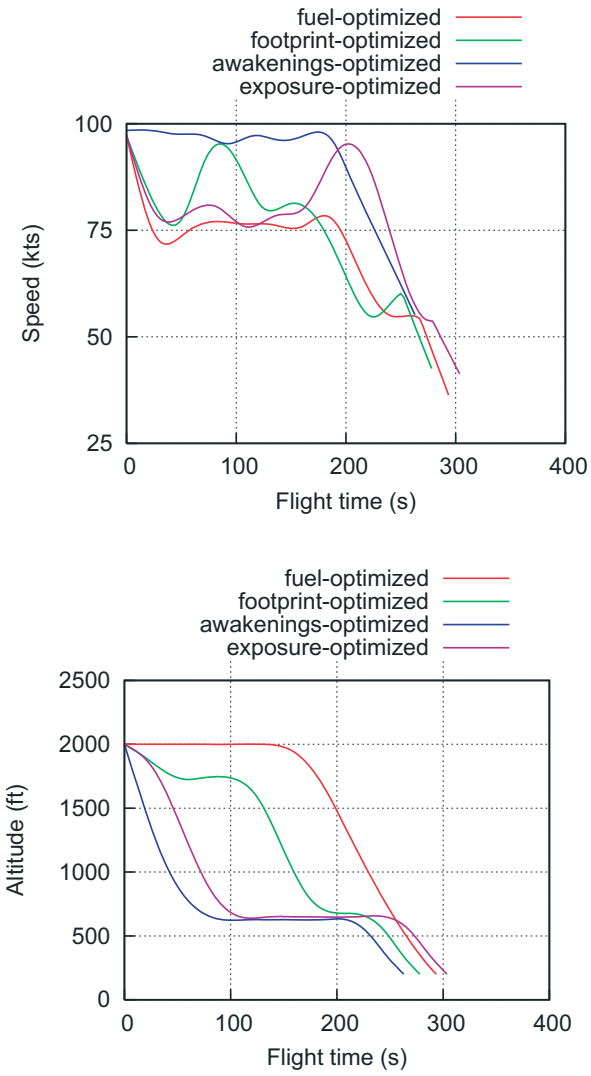

FIGURE 6. A comparison of optimal SNI approach profiles.

The airspeed and altitude profiles of the optimal trajectory solutions for cases 1 through 4 are shown in Figure 6. The corresponding ground tracks are shown in Figure 7. A comparison of the ground tracks shown in Figure 7 learns that the two solutions corresponding to a site-specific (i.e., population distribution dependent) criterion, viz., the case 2 and 3 solutions, feature very similar ground tracks that circumnavigate the most densely populated areas. The results shown in Figure 6 reveal that the altitude profiles for cases 2 and 3 are not all that different either. Indeed, in both cases altitude is reduced early during the flight to a value slightly above 500 ft, the value at which the switch to the final approach phase is made. It is conjectured that this early reduction in altitude helps to improve the lateral attenuation in the sound propagation to the side of the flight path, which is a function of the elevation angle β (see Figure 8). The reason that the trajectory levels off at an altitude some 100 ft above the glideslope intercept altitude is related to the (vertical) deceleration constraint that has been imposed. The enforced deceleration constraint precludes a rapid change of flight path angle to capture the glideslope path.

The results shown in Figure 6 also bear out that the main difference between the case 2 and 3 solutions is that in the Exposure-optimized solution (case 3), airspeed is reduced early during the flight to a value of about 75 kts, while in the Awakenings-optimized solution (case 2) speed is kept close to its initial value for the largest part of the flight.

Case 1)

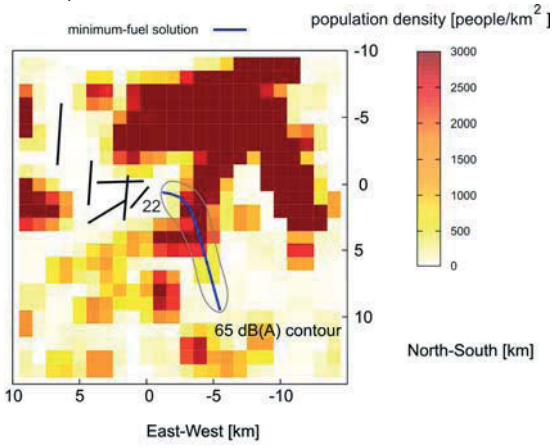

Case 2)

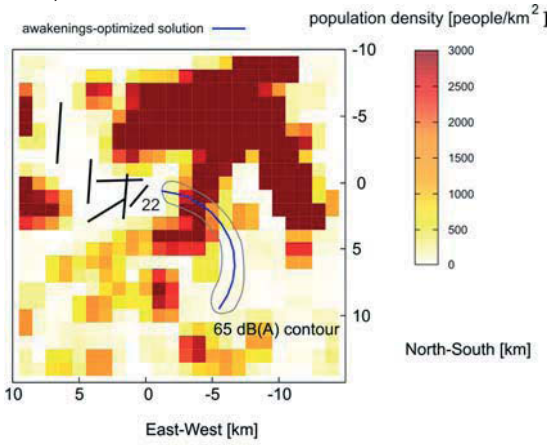

Case 3)

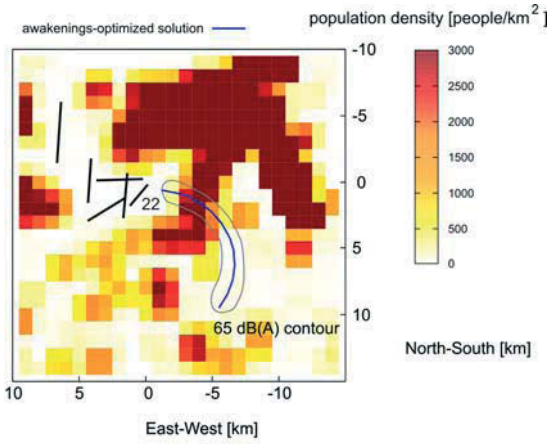

Case 4)

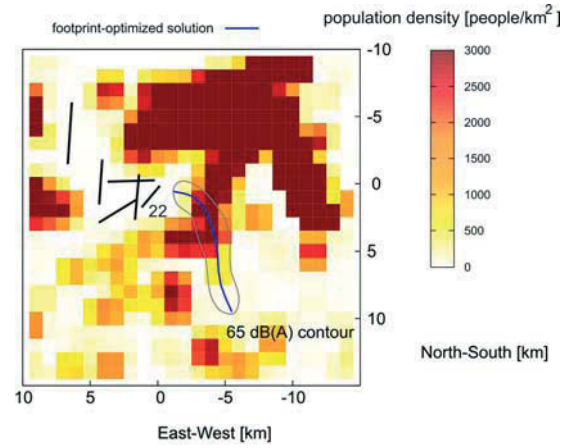

FIGURE 7. Ground tracks of optimal trajectories, with underlying population and 65 dB contour shown.

In contrast to the solutions related to the site-specific criteria, the optimal trajectories associated to the generic (i.e., population distribution independent) criteria follow a more or less direct route from the initial point to the runway (see cases 1 and 4 in Figure 7). The 65 dB(A) contours for the Fuel-optimized (case 1) and Footprint-optimized (case 4) solutions are located in relatively densely populated residential areas and, as a result, the number of people enclosed within the 65 dB(A) contour is significantly higher for the two generic cases relative to the site-specific criteria. The same holds true for the expected number of awakenings. Another striking result is that the Fuel-optimized solution features by far the largest footprint area size (see Table 2). This can most probably be attributed to the relatively low helicopter speed, resulting in an INM speed adjustment in the sound exposure levels.

A close inspection of the results in Table 2 learns that the optimal value of the glide slope angle heavily depends on the (noise) criterion that has been specified. In particular for the Awakenings-optimized solution (case 2) the value of the glide slope angle turns out to be moderate (just slightly more than 5°).

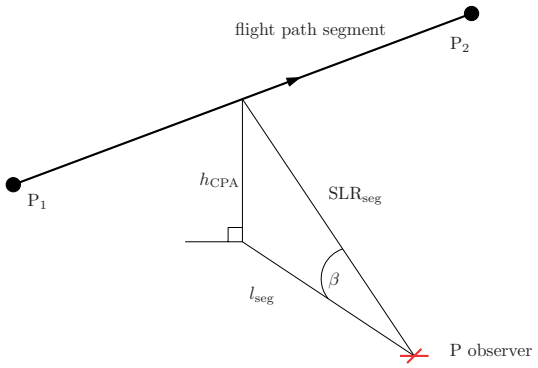

FIGURE 8. Lateral attenuation geometry: a reduction in altitude h_{CPA} leads to a reduction in elevation angle β.

FIGURE 9. Optimized SNI trajectories plotted in Google Earth

A final observation relates to the fact that the Exposure-optimized solution (case 3) results in a rather complex trajectory, exhibiting frequent and large altitude/speed variations. Yet, the achieved reduction in footprint area size relative to the site-specific solutions remains rather modest.

Figure 9 presents a screenshot of the Fuel-optimized and Awakenings-optimized SNI trajectories plotted in Google Earth. The map clearly shows that close to the airport the Awakenings-optimized solution aligns itself with a major highway. This is not really a surprising result, given the fact that the communities adjoining the highway are relatively sparsely populated.

One of the noise related cases, viz. case #2, minimize the number of expected awakenings, has also been evaluated by using INM 7.0a in the trajectory optimization.

Figure 10 shows Awakenings-optimized flight paths, calculated using INM 6.2 and INM 7.0a. Despite the markedly different noise footprints due to the different noise models, it turns out that the two resulting trajectories are not all that different. The main reason for this appears to be the fact that both solutions are largely flown at the maximum (lateral) acceleration limit of 0.05g.

FIGURE 10. A comparison of awakenings-optimized trajectories calculated using INM 6.2 and 7.0a.

TAB 2. summary of major results (INM 6.2)

Case No.	Primary Optimisation Criterion	Glide slope angle (°)	Transit time (sec)	Fuel (kg)	Number awake	Population count above 65dB(A)	Area above 65dB(A) (km^2)
1	*Fuel*	7.82	294	0.74	895	38,271	22.1
2	*Number awake*	5.13	263	0.96	477	17,932	19.1
3	*Population count above 65dB(A)*	6.87	304	0.89	509	14,010	19.1
4	*Area above 65dB(A)*	6.66	278	0.77	902	33,627	18.1

In Figure 11, the corresponding time histories of speed and altitude are shown. It is readily apparent that the altitude histories are virtually the same. The time histories of speed are somewhat different for the two solutions though. In particular, a slight drop in airspeed can be observed in the solution obtained using INM 7.0a. It is conjectured that this drop in speed is aimed at improving the turn radius in the initial phase in the trajectory. A close inspection of Figure 10 reveals that the initial turn in the INM 7.0a solution is indeed somewhat tighter in comparison to the INM 6.2 solution.

The application of the INM 7.0a acoustic model leads to on average higher predicted noise level values in the affected residential communities. As a result, the INM 7.0a solution predicts an about 29% higher value for the number of expected awakenings relative to the INM 6.2 solution.

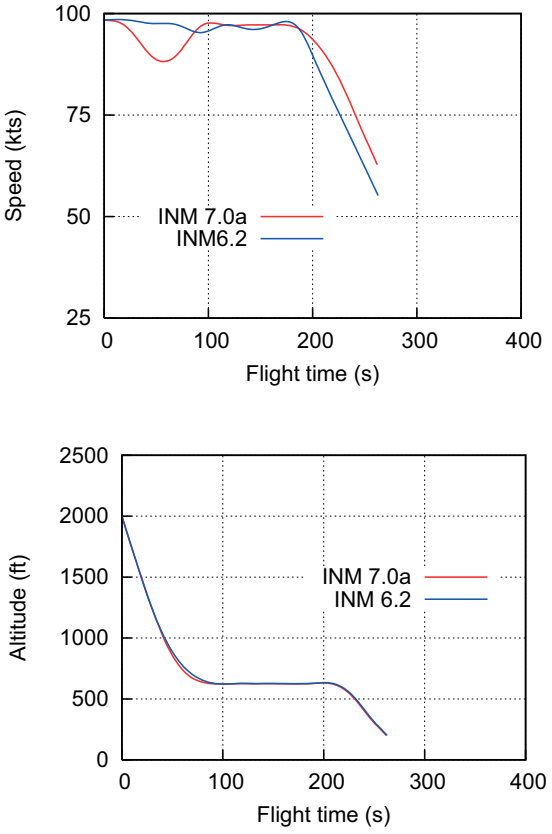

FIGURE 11. Comparison of Awakenings-optimized solutions calculated using INM 6.2 and 7.0a.

7. CONCLUSIONS

In this paper it has been demonstrated that the recently developed rotorcraft-specific version of NOISHHH proved to be very useful in the discovery of the characteristic features of noise-optimized SNI instrument approach trajectories for helicopters. An extensive parametric investigation brought to light that optimal trajectory behavior heavily depends on the specified environmental criteria. In particular it was observed that the specification of a generic environmental criterion, such as minimum noise footprint area size, may result in trajectories that can actually inflict a significant noise impact to exposed communities in the vicinity of the flight path.

In this study two different versions of the Integrated Noise Model INM, viz, version 6.2 and 7.0a were used to assess the noise impact of helicopter flyover trajectories. The noise exposure level predictions produced by the two models reveal significant differences. Nevertheless, the impact of the different models on the trajectory solution behavior turned out to be modest in the limited number of numerical experiments that were carried out. It is conjectured that this is primarily due to the fact that in the scenario considered, the optimal solutions were largely determined by the imposed acceleration constraints. A next step in the research will involve the analysis of a more extensive set of scenarios to allow assessing the characteristics of the optimal trajectory solutions.

Although results have been obtained for a limited number of hypothetical SNI procedure specifications only, NOISHHH proved to be very flexible in accommodating complex procedure specifications. This indicates that NOISHHH holds out great promise to be used as a design tool for future SNI approach procedures that enable low-noise terminal area operations.

A next step in the research will involve the implementation of a higher fidelity noise model that more accurately captures the effects of maneuvering, wind, atmospheric conditions and terrain features on the rotorcraft noise characteristics. A premier candidate for implementation is the HELENA (HELicopter Environmental Noise Analysis) tool, which is currently being developed in the framework of the European Clean Sky program [18].

References

[1] Newman, D., and Wilkins, R. “Rotorcraft Integration into the Next Generation NAS,” *Proc. of the American Helicopter Society (AHS) 54th Annual Forum*, Washington, DC, May 1998.

[2] Haverdings, H., V.d. Vorst, J., Gille, M., “Design and Execution of Piloted Simulation Tests of Steep Segmented and Curved Rotorcraft IFR Procedures at NLR, *Proc. of the European Rotorcraft Forum*, paper AO06, Maastricht, The Netherlands, September, 2006.

[3] Atkins, E. M., and Xue, M., “Noise-Sensitive Final Approach Trajectory Optimization for Runway-Independent Aircraft,” *Journal of Aerospace Computation, Information and Communication*, Vol. 1, July 2004, pp. 269–287.

[4] Xue, M., and Atkins, E. M, “Noise-Minimum Runway-Independent Aircraft Approach Design for Baltimore–Washington International Airport”, *Journal of Aircraft*, Vol. 43, No.1, 2006, pp.39-51.

[5] Conner, D.A. and Page, J.A., “A Tool for Low Noise Procedures Design and Community Noise Impact Assessment: The Rotorcraft Noise Model (RNM)“, *Proc. Of the AHS International Technical Specialists' Meeting on Advanced Rotorcraft Technology and Life Saving Activities,* Utsunomiya, Japan, 2002.

[6] Vormer, F.J., Mulder, M., van Paassen, M.M., and Mulder, J.A., “Design and Preliminary Evaluation of Segment-based Routing Methodology”, *Proc. of AIAA Guidance, Navigation, and Control Conference*, Reston, VA, 2002.

[7] Visser, H.G., “Generic and Site-Specific Criteria in the Optimization of Noise Abatement Trajectories”, *Transportation Research Part D: Transport and Environment*, Vol. 10, No. 5, 2005, pp.405-419.

[8] Visser, H.G. and Wijnen, R.A.A,, “Optimization of Noise Abatement Departure Trajectories”, *Journal of Aircraft,* Vol. 38, No.4, 2001, pp.620-627.

[9] Visser, H.G., Pavel, M. and Tang, S.F., "Optimization of Rotorcraft Simultaneous Non-Interfering Noise Abatement Approach Procedures *", Proc. of the 47th Aerospace Sciences Meeting*, Orlando, FL, U.S.A., 2009.

[10] Federal Aviation Administration, “INM 6.0 Technical Manual”, Office of Environment and Energy, Rept. FAA-AEE-02-01, 2002.

[11] Federal Aviation Administration, “Integrated Noise Model (INM) Version 7.0 Technical Manual”, Office of Environment and Energy, Rept. FAA-AEE-08-01, 2008.

[12] Federal Aviation Administration, “Policies and Procedures for Considering Environmental impacts“, FAA Order 1050.1E, March 2006.

[13] Federal Aviation Administration, “Integrated Noise Model (INM): Noise Contour Comparison: Version 7.0 vs. 6.2a“, FAA-AEE-07-01, 2007.

[14] Zhao, Y, and Chen, R.T.N., “Critical Considerations for Helicopters During Runway Takeoffs“, *Journal of Aircraft*, Vol. 32, July-August, 1995, pp. 773-781.

[15] Visser, H.G., "Optimization of Balanced Field Length Performance of Multi-Engine Helicopters", *Journal of Aircraft*, Vol. 37, July-August, 2000, pp. 598-605.

[16] Leishman, J.G., "Principles of Helicopter Aerodynamics", Cambridge University Press, Cambridge, 2000.

[17] Federal Aviation Administration, "Fitchburg Municipal Airport Noise Measurement Study: Summary of Measurements, Data and Analysis", Office of Environment and Energy, Rept. FAA-AEE-05-01, 2005

[18] http://www.rotorsales.com/News/060508_1.htm